Complexation leaching of critical and strategic metals from nickel converter slag using organic acids

Bona Lim [a], Richard Diaz Alorro [a,*], Mark Aylmore [b], David Grimsey [c]

[a] *Western Australian School of Mines: Minerals, Energy and Chemical Engineering, Curtin University, Bentley, WA 6102, Australia*
[b] *John de Laeter Centre, Faculty of Science & Engineering, Curtin University, Bentley, WA 6102, Australia*
[c] *Nickel West Australia, BHP, Feysville, WA 6431, Australia*

ABSTRACT

Nickel converter slag is a waste product formed during the converting process in nickel production. In recent times the processing of nickel converter slag has gained attention as a secondary source of cobalt (Co) and nickel (Ni). Nickel and cobalt are considered critical and strategic metals that are essential for nations' economy and defence, as well as high-technology industry. In particular, Co and Ni can be utilised in the batteries, superalloys, and automobiles. Extraction of critical and strategic metals from slag can be categorised as technospheric mining. In this study, the slag was characterised using combination of XRF, XRD, ICP-OES, FESEM and TIMA for better understanding of deportment of Ni and Co and texture of Ni converter (CV) slag. Complexation leaching by using a combination of citric acid and EDTA was undertaken to extraction by using the leaching agent and complexing agent. The preliminary test showed the most promising result. The leaching experiment was carried out with various parameters such as the reagent concentration, temperature, particle size, and pulp density. The optimum condition for extracting Co and Ni from CV slag is following; citric acid 1 M, EDTA 0.3 M, 80 °C, 6 hr, pulp density 2.5% (w/v), − 75 μm and 250 rpm, which recovered 85.29% of Co and 59.85% of Ni.

1. Introduction

Cobalt (Co) and nickel (Ni) are considered critical and strategic materials since they are facing an increasing demand with projected supply risk and limited substitution (Simandl et al. 2015). Owing to their unique properties, Co and Ni are widely used in various industries such as automobile, aerospace, communication, manufacturing, and high- and clean-technology (Ortego et al. 2020; Simandl et al. 2015). Co has ferromagnetic properties with high temperature resistance, which enables the production of permanent magnet. In addition, Co has variable oxidation states and high metal hardness (Dehaine et al. 2021). These properties of Co attracted many applications such as superalloys for aircraft engines, batteries, catalysts, and carbides (Sarker et al. 2022). The value of Co is extraordinary since Co is mainly produced as a by-product of copper (Cu) or Ni. Consequently, the price of Co increased by 17% from 2016 to 2020 (USGS, 2021). Ni is widely known for anti-corrosion properties, thus used in many industrial applications such as alloys, electronics, batteries, and catalysts. Thus, industrial wastes commonly contain Ni, which should be recovered to prevent a negative impact on the environment and ecosystem (Coman et al. 2013). The

increasing demand of Ni resulted the rise of Ni's price by 31 % from 2016 to 2020 (USGS, 2021). Due to significance of critical and strategic metals such as Ni and Co, there has been an increasing interest in extraction of critical and strategic metals from secondary sources (Gunn 2013).

Conventionally Ni and Co are recovered by smelting that produces a nickel matte and slag. Two types of slag are generated in the process from the flash furnace (FF) and converter (CV). Both types of slag contain valuable Co and Ni. The recovery of Co from the smelter rarely exceeds 60 % because Co has similar properties with iron (Fe) in pyrometallurgy (Grimsey 1992). The process includes dilution of CV slag by sending it back to the flash furnace, however, due to poor dilution and separation of slag and matte, the nickel matte is captured in FF and CV slag, which is a major cause of Ni loss (Wang et al. 2018). The dilution of CV slag to flash furnace affects the furnace by decreasing the feed and increasing the impurities (Perederiy et al. 2011).

Extraction of critical and strategic metals from slag can be categorised as technospheric mining(Lim and Alorro 2021). Technospheric stocks also include mine waste, e-waste, landfill, and products which are currently being used and will become waste in near future (Johansson

---

Table 1
Chemical composition of CV slag by XRF and ICP-OES.

Mass %	Al	Fe	Si	Mg	S	Ni	Co	Cu
XRF	0.10	55.52	11.41	0.07	0.86	1.2	0.59	0.07
ICP	0.09	58.42	–	0.09	–	1.27	0.59	0.13

et al. 2013). Technospheric mining incorporates the life cycle of materials and provides an appealing opportunity for mining industry by waste valorisation (Ichlas et al. 2022). Previous studies on the recovery of metal values from nickel slag have used pyrometallurgical or high-pressure oxidative leaching methods (Li et al. 2009; Wang et al. 2018).

This study investigated a hydrometallurgical complexation leaching approach to recover Co and Ni directly from nickel converter slag under ambient temperature and pressure conditions. Complexation leaching involves dissolving target elements by forming a stable complex with a suitable complexing reagent. Complexation leaching has several advantages such as selectivity for target metals, low impact on environment by using organic acids, and recycling of the complexing agents where possibility (Goel et al. 2009; Nayaka et al. 2015). Extraction of critical and strategic metals from nickel converter slag using complexation leaching has not been examined. In this study, citric acid as a leaching agent and ethylenediaminetetraacetic acid (EDTA) as a complexing agent were chosen since citric acid is a strong organic acid and EDTA forms highly stable Co and Ni complexes. The stability constants of metal ions with EDTA are following; Co^{3+} 41.4 > Mn^{3+} 25.3 > Fe^{3+} 25 > Cr^{3+} 23.4 > Ti^{3+} 21.3 > Cu^{2+} 18.8 > Ni^{2+} 18.4 > Co^{2+} 16.4 > Fe^{2+} 14.3 (Smith and Martell 1987). This study can prove the potential of complexation leaching on nickel converter slag.

In this study, the effect of reagent concentration (citric acid and EDTA), temperature, particle size and pulp density on Ni and Co extraction were examined. The mineralogical characteristics of both the slag feed and leached residue were characterised. To understand the effect of complexation leaching, species diagram of complexes was created, and the leaching residues were analysed by the microscopy.

2. Experimental

2.1. Materials

The nickel converter slag was provided by Kalgoorlie nickel smelter and collected from a historic pile. The slag was prepared by a combination of jaw crushing, cone crushing and rod milling, followed by pulverised and sieved to produce a sample that passed 75 μm. All the samples used in this study were under 75 μm unless specified. The reagents used for complexation leaching were citric acid (Sigma-Aldrich, 100% grade) and ethylenediaminetetraacetic acid (EDTA) (Rowe Scientific, greater than99% grade).

2.2. Methods

A combination of analytical methods was utilised to understand the characteristics of nickel converter slag and leaching residues. X-Ray fluorescence (XRF, PANAnalytical, UK), X-Ray Diffraction (XRD, PAN-Analytical, UK), Field Emission Scanning Electron Microscopy (FESEM, Clara, Tescan), and TESCAN Integrated Mineral Analyser (TIMA GM, Tescan) were used. Inductively Coupled Plasma Optical Emission Spectroscopy (5100 ICP-OES, Agilent) was used to identify Co, Ni and other elements in the leaching solution.

The leaching experiments were conducted with a 500 mL three-check flask on a heating mantle, attached to a reflux condenser, a thermometer, and a mechanical stirrer. In most tests the particle size (P_{100} = -75 μm), stirring rate (250 rpm), and solid–liquid ratio (10%) were fixed unless specified. The experiments were performed using a
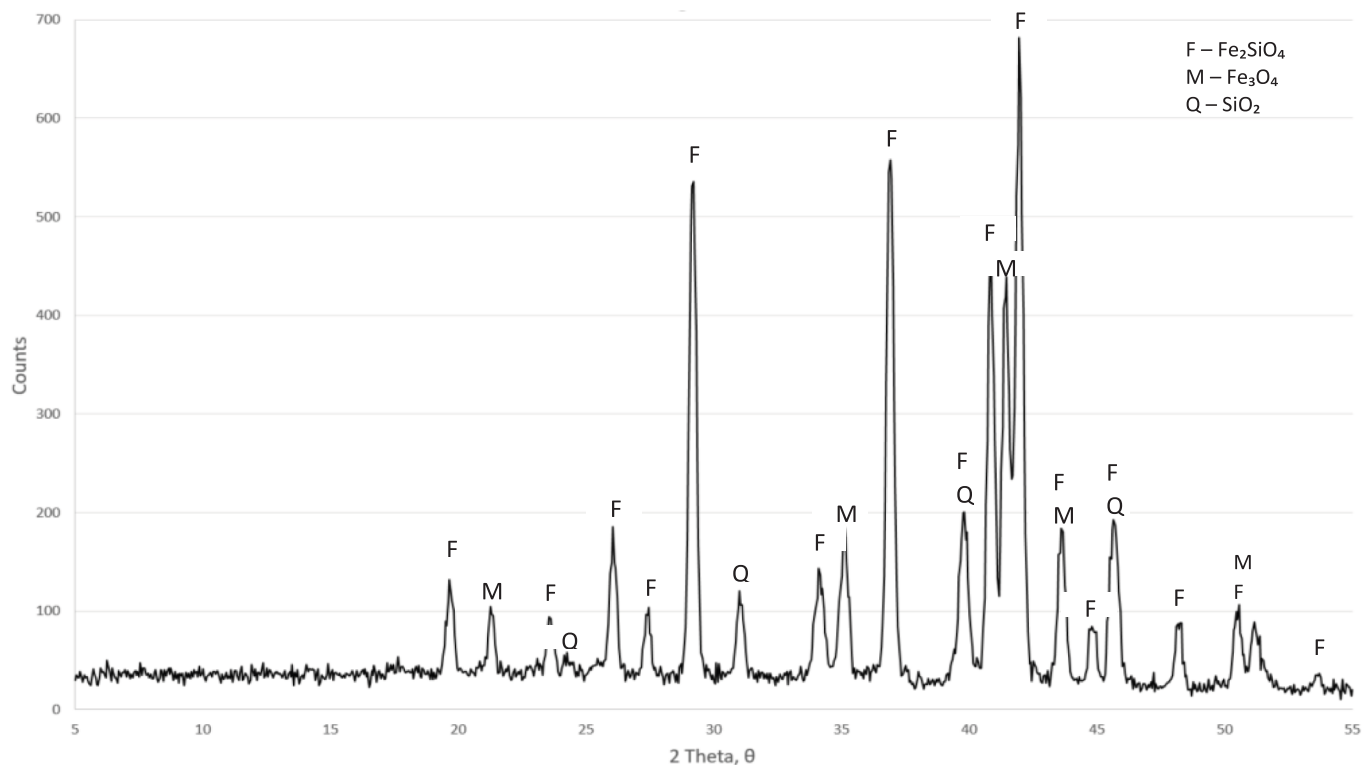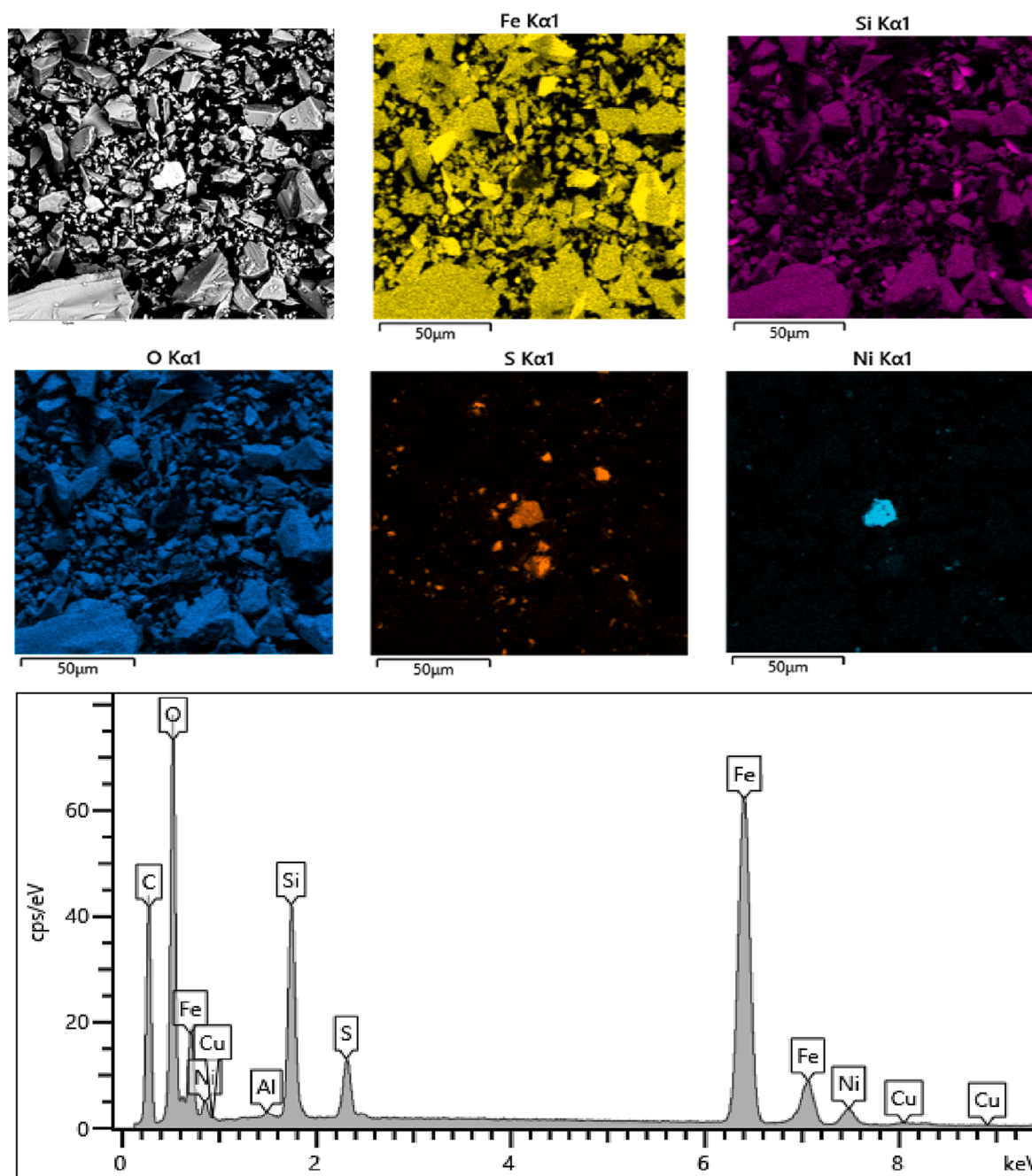

Fig. 1. XRD spectrum of CV slag.

Fig. 2. Backscatter electron (BSE) image, elemental map, and spectrum of CV slag by FESEM.

One Variable at A Time (OVAT) experimental plan. Repeat experiments were conducted for anomalous results for confirmation and reliability. Mass balance calculations to determine the leaching recovery were confirmed by analysing the leaching solutions as well as by acid digestion of leaching residue.

3. Results and discussion

3.1. Slag characterisation

Chemical composition of the CV slag is present in Table 1. The measurements obtained from XRF were converted from the oxides to the elements. Iron (Fe) and silica (Si) are the main components of the CV slag. CV slag contains 1.2% of Ni and 0.59% of Co. An aqua regia digest was conducted and established more than 90% of Co and Ni extracted

from CV slag (results not shown). In the process, sampling and/or dilution could have caused the marginal differences in the results.

XRD scan of CV slag is shown in Fig. 1. The major phases of CV slag are fayalite (Fe_2SiO_4), hematite or magnetite (Fe_3O_4), and quartz (SiO_2). No Co and Ni phases were abundant enough to be detected. Ni and Co is known to exist in the slag as chemically bound oxide + s in fayalite (Baghalha et al. 2007; Li et al. 2008), as Co and Ni ferrites ($CoFe_2O_4$ and $NiFe_2O_4$) (Li et al. 2009; Huang et al. 2015), or Ni and Co bearing sulfides (Li et al. 2009). Ni can also be found in entrapped matte as a discrete mineral phase.

The back scattered electron (BSE) image, elemental map, and energy dispersive spectrum of CV slag particles are shown in Fig. 2. The elemental maps and energy dispersive spectrum of the CV slag indicate high content of Fe, Si and O. The surfaces of the fragmented fayalite particles of CV slag are smooth. In the middle of a BSE image, the bright
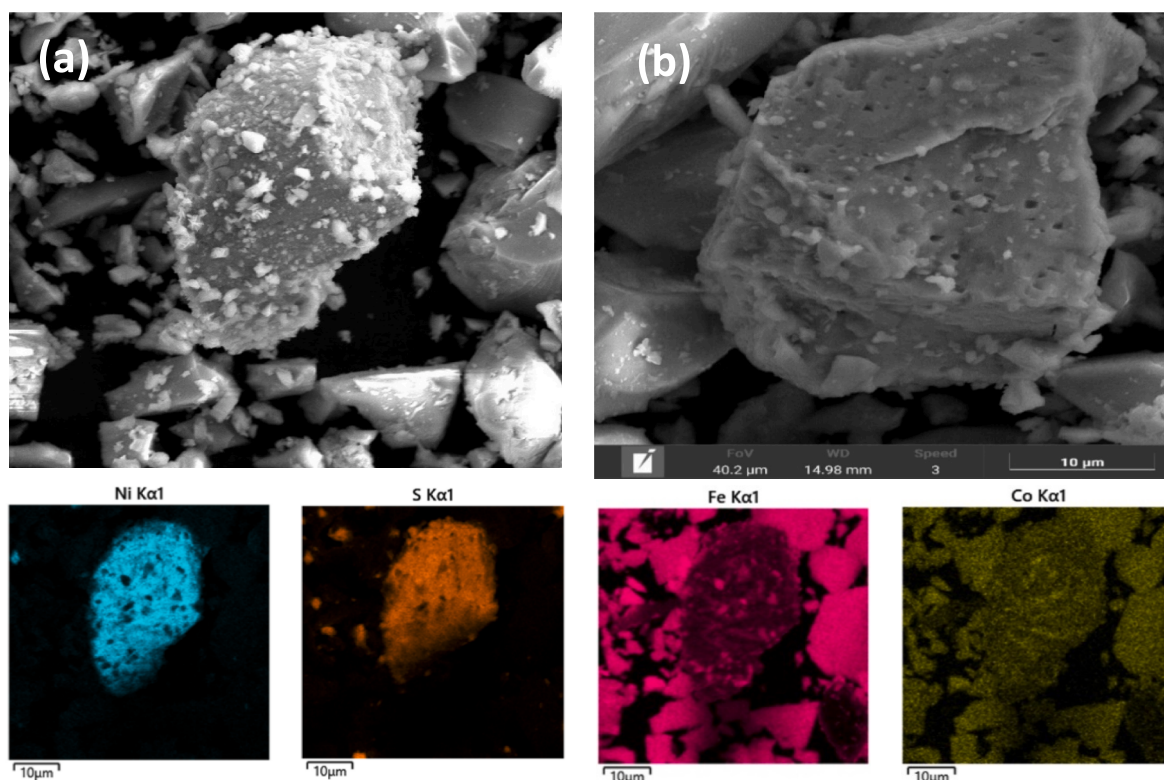
Fig. 3. Electron micrograph images of entrapped nickel matte (a) with elemental distribution maps and particle with porous structure (b) in CV slag.

Table 2
Phase abundance in CV slag by TIMA.

Primary Phases	%
Fayalite phase	0.00
Fayalite phase – high Fe	75.66
Fayalite Fe Mg rich	0.00
Fayalite no Mg	0.10
Fayalite high Ca	0.01
Hematite/Magnetite	21.50
Quartz	0.51
Pyrrhotite	0.72
Unclassified	1.35
Total	99.85

particle is the nickel sulphide that is also confirmed from the elemental map (regions high in Ni and S). The presence of pyrite was observed with the regions high in Fe and S. The spectrum presents Ni, Cu, Al, and S. Co was not detected due to low grade. Carbon (C) is from the background tape and coating used to prevent image charging.

Fig. 3 shows the detailed particles of CV slag, which is a nickel matte (a) and a particle with porous structure (b). The elemental map of the nickel sulfide shows that the small sulfide particles are covering Ni, though Ni has some exposed surface, which will be favourable for chemical reaction. The particles around the nickel matte show high Fe content and Co is dispersed throughout the slag including Ni matte.

Even though it is rare to find the particles with poles from the original slag sample, the poles on the particle are shaped in round or square. The porosity is undoubtedly generated when air bubbles escaped the particle during the smelting and converting process. The average diameter of the poles is 0.70 μm.

Phase abundance and mineral associations in the CV slag a were analysed by TIMA scanning electron microscopy technique. Table 2 shows that the CV slag consists of 75.66 wt% fayalite with hematite/magnetite (21.5%) and minor pyrrhotite (FeS) (0.72 wt%), which make up 97 % of the slag. A cross section mineral composition map shown in

Fig. 4 indicate that the fayalite particles are impregnated with iron oxide particles (Fig. 4a). Nickel sulphide in CV slag is detected as pentlandite $((Fe,Ni)_9 S_8)$ (Fig. 4b), which also includes Co in the mineral structure (Shen et al. 2008). Pyrrhotite is also found associated with pentlandite.

In summary, the major phases in the slag are fayalite, hematite/magnetite, and quartz. Most of Ni is shown as sulfide since nickel matte is entrapped in the slag. It is assumed that fayalite associates with Ni and Co, thus a certain amount of Ni and Co can exist in the oxide form. The amount of Ni in olivine varies and depends on the place where it is found, varying between 0 and 0.5 wt% of Ni as well (Thompson et al., 1984). From FESEM images, nickel sulfide is found to be relatively well-liberated under 75 μm. Thus, dissolution of fayalite to extract Ni and Co is the main aim of leaching.

3.2. Leaching tests

3.2.1. Effect of citric acid concentration

Fig. 5 (a) and (b) show the effect of citric acid concentration on the extraction of Co, Ni, and other elements with the fixed conditions of EDTA 0.3 M, 60 °C, 6hr, and PD 10%. Purple lines with dots show the extraction rate of Co with different concentrations of citric acid in Fig. 5 (a). Out of the three citric acid concentrations examined, 1 M of citric acid extracted the fastest at 1 h by dissolving 47% of Co. Yellow lines with triangles represent the extraction rates of Ni, and also indicated that 1 M of citric acid dissolved the most Ni. Therefore, 1 M of citric acid was chosen for further experiment. At the same time, less than 60% of Fe and Si were also leached in Fig. 5 (b) with citric 1 M and EDTA 0.3 M. After 1 h, Fe seems the trend of precipitation in the solution, which might have affected the dissolution of Co. Another theory of decreased leaching recovery of Fe is that amorphous silicates coated fayalite and other particles and prevented further dissolution since Si and Al continued to be leached after 1 h.

3.2.2. Effect of EDTA concentration

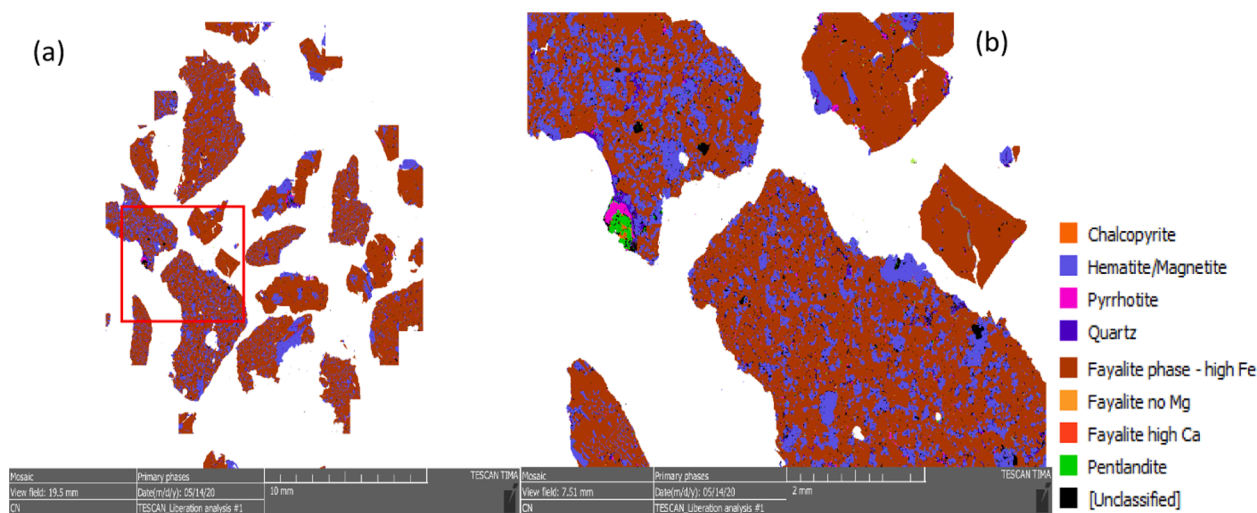Fig. 6 (a) and (b) reveals the effects of EDTA concentration (0.1 M to

Fig. 4. TIMA mineral composition map shows cross section of CV slag particles; (a) Fayalite particles with fine hematite grains and (b) expanded image (red square area) showing coarse pentlandite located adjacent to fayalite particle. (For interpretation of the references to colour in this figure legend, the reader is referred to the web version of this article.)
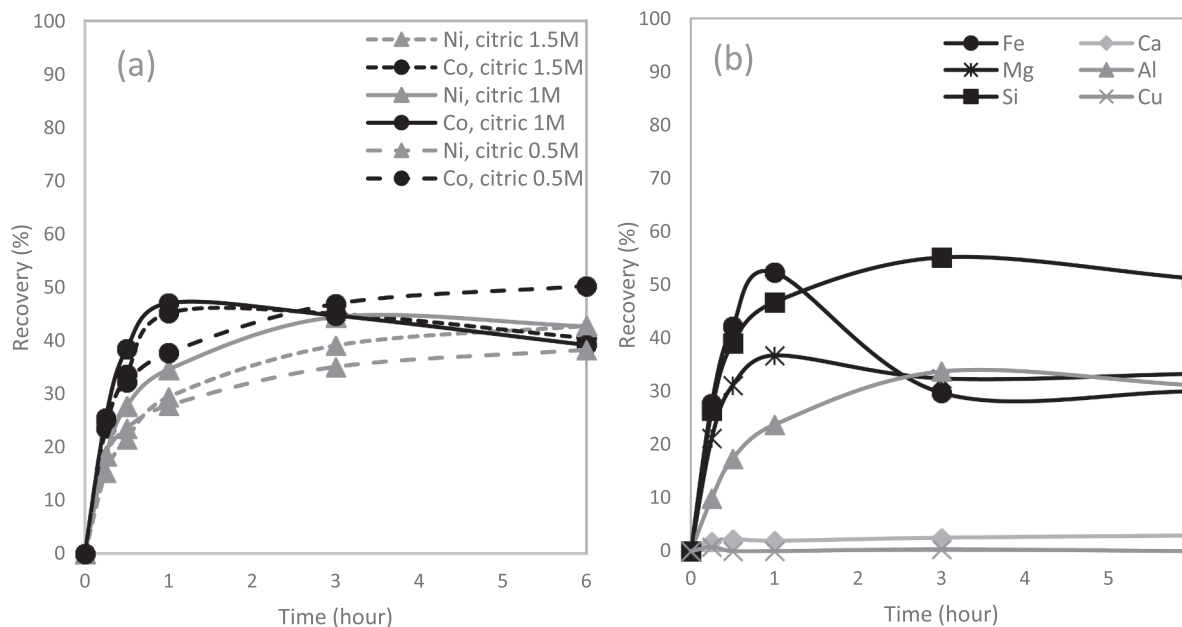

Fig. 5. The effect of citric acid concentration (0.5, 1 and 1.5 M) on the dissolution of Co and Ni (a) and the dissolution of other elements (1 M) (b). (Fixed conditions of EDTA 0.3 M, 60 °C, 10% solids)).

0.7 M) on the leaching of Co and Ni respectively o. The citric acid 1 M, 60 °C, 6 h, PD 10% (w/v), and agitation speed of 250 rpm. From Fig. 6 (a), the reaction rate until 1hr is fast for all the conditions, though 0.1 M might have been insufficient for complexation. Also, Co with 0.3 M EDTA seemed plateau after 0.5 h. The highest extraction of Co was 51.25% after 6 h with EDTA 0.5 M. For Ni recovery in Fig. 6 (b), EDTA 0.3 M extracted 50.21% after 6 hr. According to the mineralogy in 3.1., dissolving Fe to break down the structure and liberate the target elements seems mandatory to extract Co and Ni. For further experiments, 0.3 M of EDTA was chosen considering both Co and Ni recoveries.

To investigate the selectivity and correlation in dissolution between Fe and Co & Ni, specifically with EDTA 0.3 M, the molar ratio of the [Ni]/[Fe] and [Co]/[Fe] during leaching, was examined and is presented in Fig. 7. The ratio of [Co]/[Fe] is close to constant over the leaching period, which indicates that the dissolution of Fe follows extraction of Co. This confirms that dissolution of Co depends on the Co-

bearing fayalite. The ratio of [Ni]/[Fe] is independent of each other. It is likely that Ni is coming from the dissolution of exposed pentlandite grains as seen in Fig. 4. Thus, it is confirmed that dissolution of fayalite is required to liberate Co from the CV slag, whereas dissolution of nickel sulphides is the key parameter for recovery of Ni.

3.2.3. Effect of temperature

Temperature is an important factor in the leaching due to the effect on the dissolution as well as the operating cost. Controlling the suitable temperature in the complexation leaching is crucial since it can affect the dissolution of unwanted elements, which might interfere the filtration significantly (Habashi 1993). The parameters for the experiment were citric acid 1 M, EDTA 0.3 M, 6 h, PD 10% (w/v) and 250 rpm.

Increasing the temperature up to 90 °C created minor differences in the extraction rates of Co and Ni from CV slag as shown in Fig. 8 (a) and (b). The highest recovery of Co was 52.04% at 1 h with 90 °C. For Ni, it
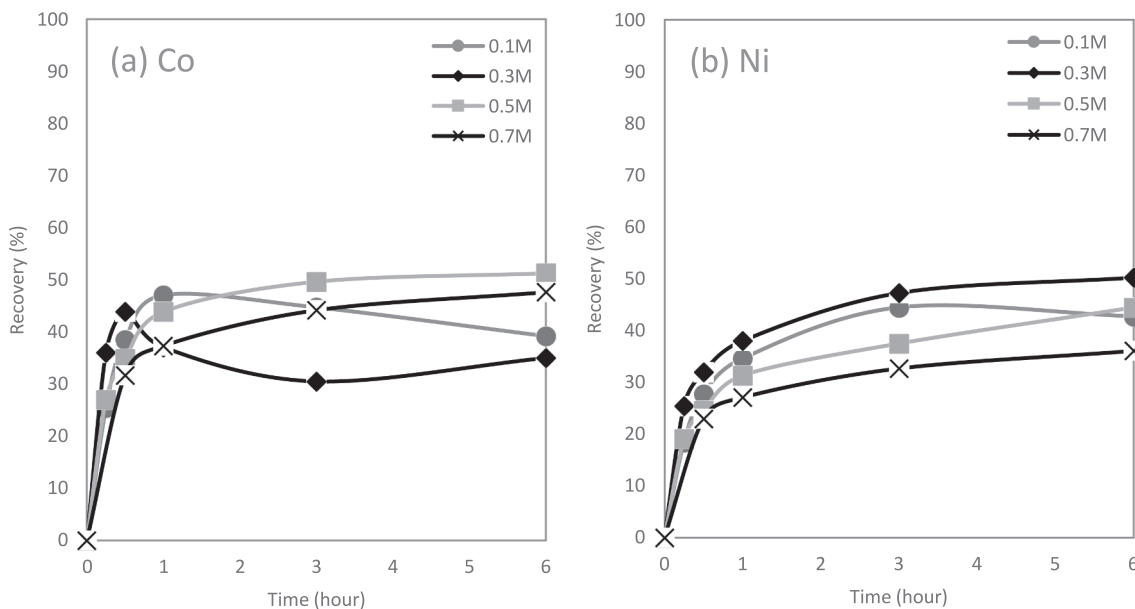
Fig. 6. The effect of EDTA concentrations (0.1 – 0.7 M) on the dissolution of Co (a) and Ni (b).
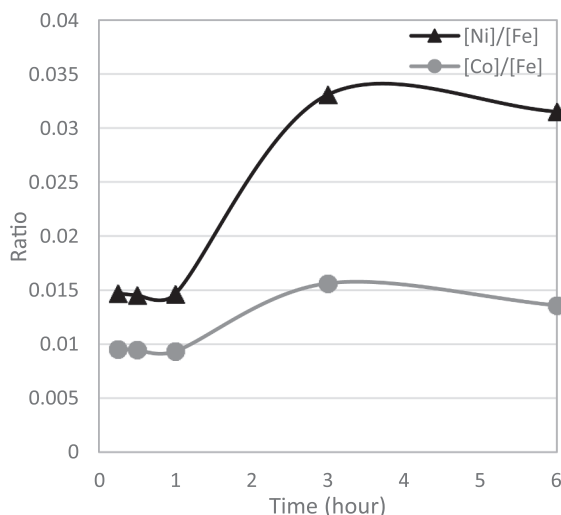

Fig. 7. The molar ratio of [Ni]/[Fe] and [Co]/[Fe].

was 51.16 % at 90 °C after 6 h. In Fig. 8 (a), increasing the temperature has minor effect in extraction of Co, for example 2% of recovery was increased at 1hr from 60 to 90 °C, and the recovery rates are in a similar range at 6 hr from 25 to 90 °C. For Ni, increasing the temperature and extending the time of leaching clearly show more extraction in the solution in Fig. 8 (b). Though it is the highest recovery at 90 °C, increasing the temperature did not meet the expectation, thus, further experiments were conducted at 80 °C to minimise the precipitation of the target elements.

3.2.4. Effect of particle size

Comminution takes up to the biggest part in the processing budget due to usage of significant amount of energy, thus particle size must be considered as one of the important parameters in the leaching. Having the optimum particle size can save energy, screen unwanted minerals and make sure liberation of the target elements (Ma and Houser 2014). Particle sizes were varied to −100 + 75, −75 + 38, and −38 μm, and the fixed conditions were citric acid 1 M, EDTA 0.3 M, 80 °C, 6 h, PD 10% (w/v), and 250 rpm.

In Fig. 9, the highest recovery of Fe, Ni and Co was achieved from the −38 μm sample, with extractions of 36.5%, 57%, and 60.36% respectively. The error bars in Fig. 9 represents the decreasing rate of extraction during the experiment. For example, the recovery of Fe was the highest at 1hr by 43.35% then decreased to 36.5% at 6 hr. It can be expected that depending on the pH of the solution during leaching, the precipitation of Fe might be a cause of decreasing recovery or significant dissolution of other elements might have caused the decrease in a grade of Fe in the leaching solution (Prasetyo et al. 2021). The effect was prominent in the finest particle of −38 μm. Co also showed the similar behaviour as Fe, which can be assumed by two possible reasons; it was affected by the precipitation along with Fe. Since the nature of slag's mineralogy shows that Co is captured in the fayalite, it seems dissolution of Fe was dominant in the fine particle to extract the other elements, and the reagents were also consumed by the liberated impurities. The highest recovery of Ni, as well, can be explained by the exposed surface from the nickel sulphide by fine grinding.

3.2.5. Effect of pulp density

The effect of pulp density on the extraction of Co and Ni is shown in Fig. 5. Adjusting the optimum pulp density is vital for mass transfer, metals dissolution and reagent consumption. Higher pulp density can yield higher Ni and Co concentrations in the solution though precipitation might occur in the solution when saturated (Huang et al. 2015). Pulp density was varied from 2.5% to 15%, for example, 30 g / 300 mL is 10%. Other conditions were fixed to citric acid 1 M, EDTA 0.3 M, 80 °C, 6 h, – 75 μm and 250 rpm.

The pulp density 2.5% resulted in the highest recovery of Co and Ni after 6 h, 85.29 % and 59.85% respectively. With Ni's recovery, the difference in Ni extraction between 2.5 and 5 % pulp density is small. In contrast Co, extraction increased by 10%. The Ni recovery is more susceptible to liberation of the nickel sulfide whereas the Co recovery is dependent on the dissolution of fayalite. After 3 h of experiment with 15% pulp density, severe silica gelation occurred, so the solution and residue samples at 6 hr were unable for collection.

3.3. Species diagram

To aid in the interpretation of the experiments, Pourbaix diagrams of the Ni-EDTA, Co-EDTA, Ni-citrate, and Co-citrate complexes were examined and are shown in Figs. 11 to 14. Once Eh and pH were
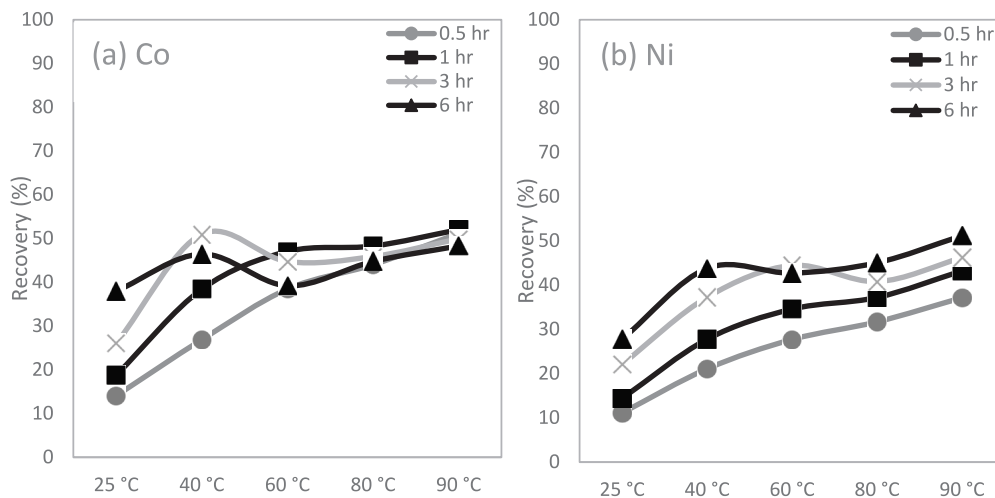
Fig. 8. The effect of temperature on the extraction of Co (a) and Ni (b).
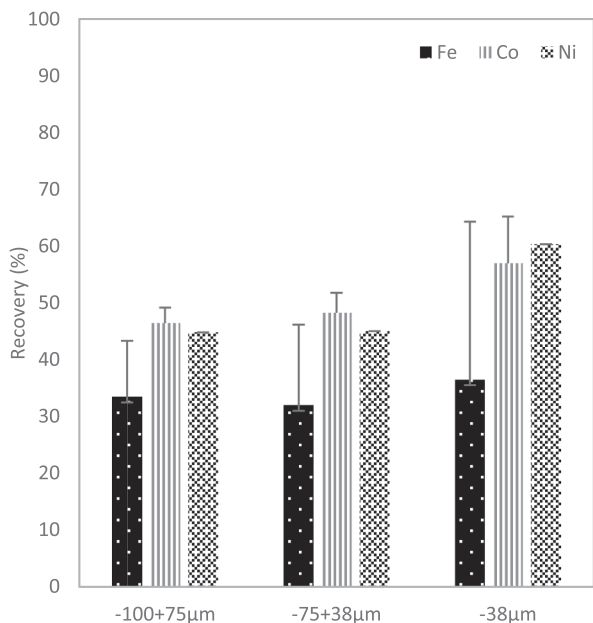

Fig. 9. The effect of particle size on the leaching recovery of Co and Ni.

measured from the leaching solution, the Eh-pH diagram enables to identify the complexes in the solution. Eh-pH diagrams were created by using the software Medusa with Hydra database.

The optimum condition above in Fig. 10 with PD 2.5% were used to create the diagrams and will be used to interpret the diagrams. The initial pH and final pH of the experiment was 2.56 and 2.39. Eh was initially 0.29 V and lastly 0.1 V. With this information, it can be expected that Ni and Co exist in the leachate as Ni(HEDTA)$^-$ and Co(HEDTA)$^-$. As discussed above in 3.2., Ni and Co complexes are known to from stable stability as the diagrams show various forms of complexes in the Eh-pH range. pH 2 – 3 is the ideal because acidic environment breaks the fayalite lattice and nickel matte to expose Co and Ni, and at the same time, Ni and Co can form complexes with EDTA. However, pH 3 – 4 is known to precipitate Fe (Meruane and Vargas 2003), thus delicate control of pH with the amount of acid was required.

It is worth to mention that to create the Ni-EDTA and Co-EDTA Eh-pH diagrams in Figs. 11 and 12 using the software, citric acid 1 M and EDTA 0.3 M along with the concentrations of Ni and Co were inputted but citrate complexes were not shown in the diagram due to the strong

affinity of EDTA with Co and Ni. Thus, for Figs. 13 and 14, the concentration of EDTA was removed to reveal the citrate complexes with Co and Ni. A possible theory is that when there is no more EDTA available in the solution due to consumption by other elements, citrates will be able to form the complexes with Co and Ni to continue the dissolution. So, citric acid can perform as a leaching agent as well as a complexing agent in the leaching. From the pH and Eh range mentioned above, Ni (Hcit) and Co(Hcit) can be formed in the solution. The stability constants of citrates with Co and Ni are lower than the ones from EDTA, however, it is sufficient to form the stable complexes; Ca^{2+} 23.93 > Al^{3+} 19.81 > Cu^{2+} 19.56 > Fe^{2+} 13.61 > Fe^{3+} 13.35 > Ni^{2+} 5.19 > Co^{2+} 4.74 (Markich and Brown 1999; Bastug et al. 2007).

3.4. Residue characterisation

The solid residues from complexation leaching of CV slag were analysed by FESEM. Fig. 15 shows the BSE images of the particles and spectrum of the residue. The BSE images clearly reveal that the CV slag is severely fragmented by leaching. The bright particles in Fig. 15(a) are high Fe fayalite, and the destructed particles are hematite. The particles in Fig. 15(b) and (c) are the residual fayalite after leaching, which was also attacked by the reagents. Compared to the original sample in Fig. 2, the counts of Fe, Si, S and Ni were significantly reduced but O stayed about the same. It can be suspected that dissolved Fe precipitated as hematite, which was shown in Fig. 5 (b) that after 1hr of leaching, Fe content in the solution decreased. It is also confirmed by Fig. 15 below that hematite particles were easily found by FESEM, even considering the CV slag before leaching contained 21.5% of hematite.

4. Conclusions

Current procedure sends CV slag back to the circuit to flash furnace to recover further Ni and Co, however, due to the poor dilution and separation between slag and matte, the recovery rate of Ni and Co do not exceed 60%. This study has shown that the complexation leaching using organic acids can extract Co and Ni from nickel converter slag. The optimum condition was citric acid 1 M, EDTA 0.3 M, 80 °C, PD 2.5%, 6 h, – 75 μm and 250 rpm, and 85.29% of Co and 59.85% of Ni were extracted. Extraction of other elements were monitored, and it shows that Fe, Mg, Si, and Al also consume the reagents in the leaching.

As expected, dissolution of Fe is the key parameter for leaching as the correlation between Co and Fe was almost linear. In the meantime, extraction of Ni was affected by dissolution of sulfur, which also limited the complete extraction of Ni in this system. In general, extraction of Ni and Co happened fast, and after 1hr of leaching, the extraction rate tends
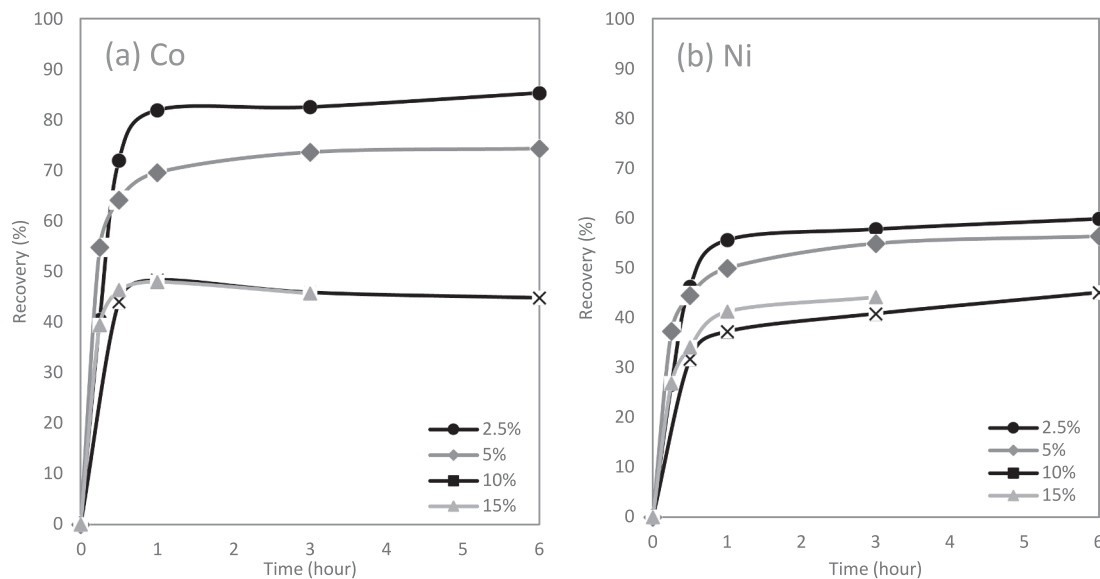
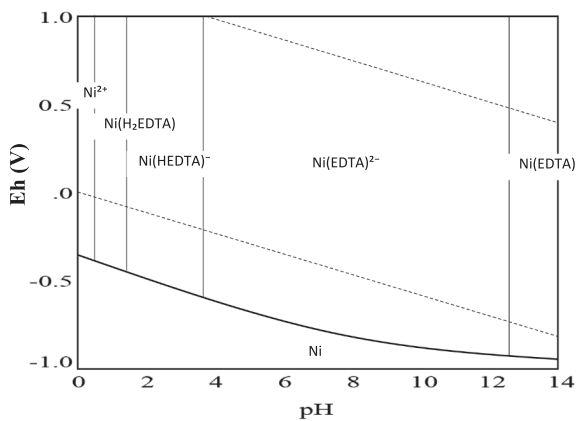**Fig. 10.** The effect of pulp density (2.5, 5, 10 and 15%) on the extraction of Co (a) and Ni (b).
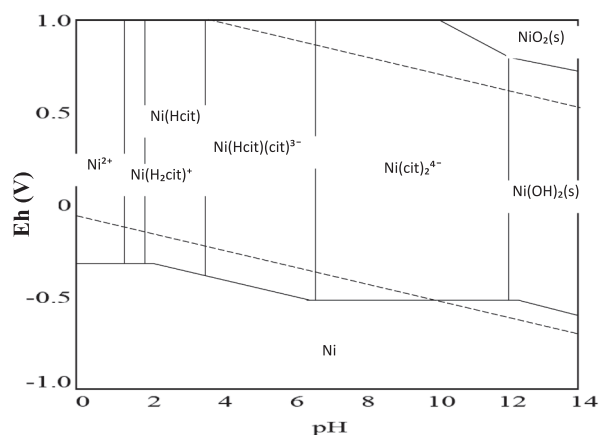

Fig. 11. Eh-pH diagram of Ni-EDTA complexes.

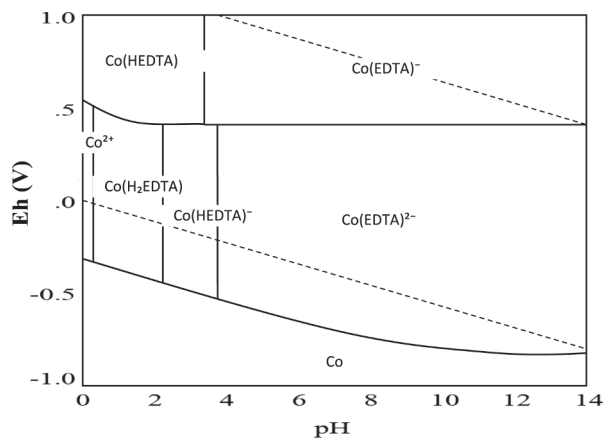**Fig. 13.** Eh-pH diagram of Ni-citrate complexes.

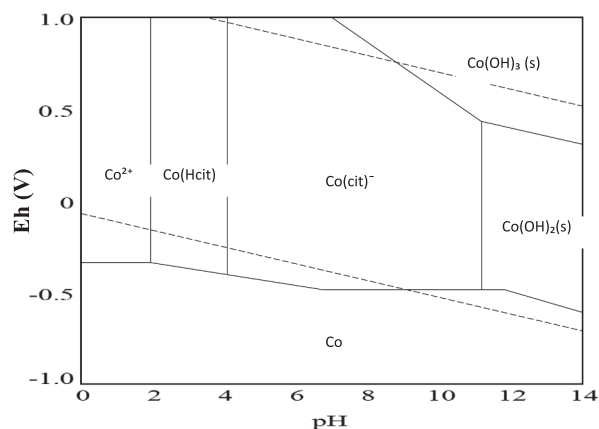**Fig. 12.** Eh-pH diagram of Co-EDTA complexes.

Fig. 14. Eh-pH diagram of Co-citrate complexes.

to reach the plateau. Leaching residues were analysed for further understanding of mechanism. After complexation leaching of nickel converter slag, a significant amount of hematite was found. Original sample contained 21.50% of hematite/magnetite and 75.66% of high Fe fayalite. It can be suspected that the dissolved Fe from fayalite precipitated as hematite. Also, the analysis of residue showed that the amount of Fe,
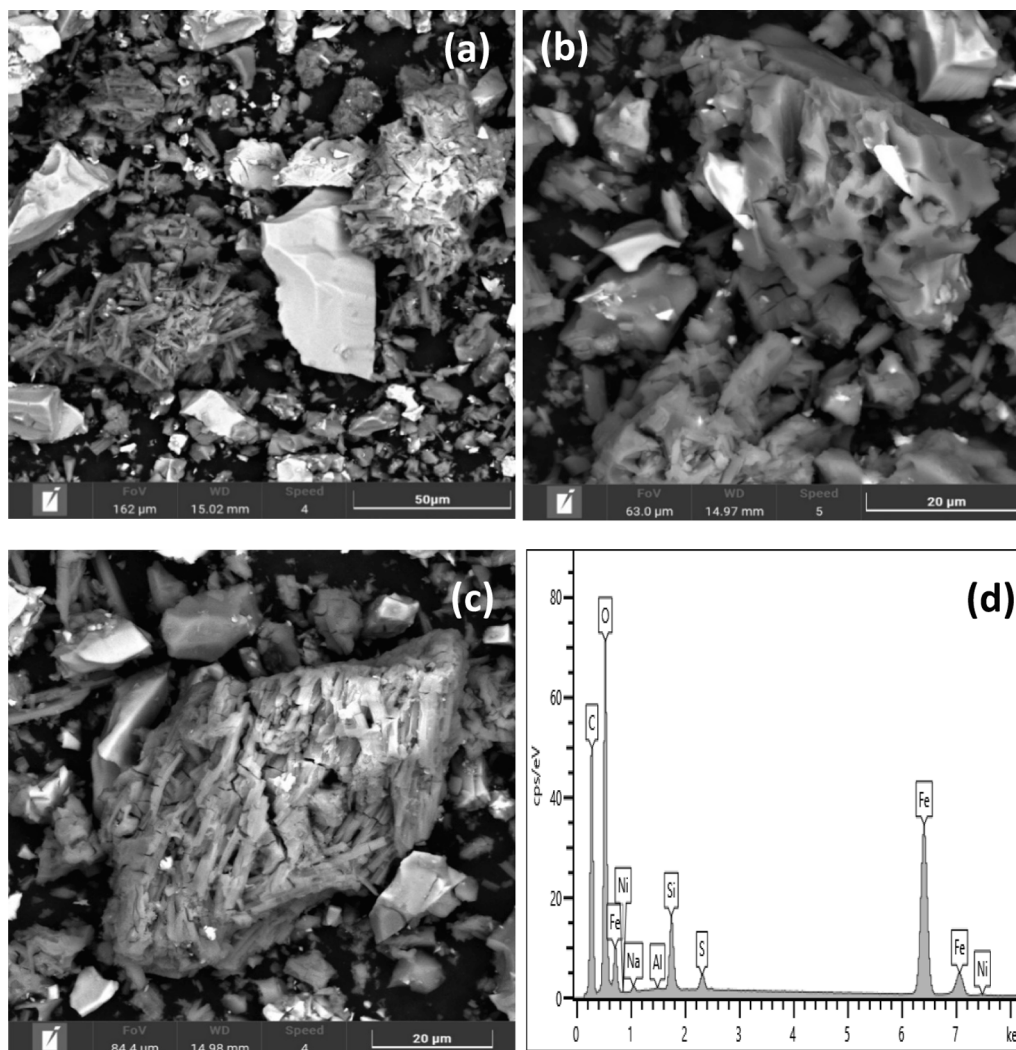
Fig. 15. BSE images of residue (a) and hematite (b) and residue particle (c)'s spectrum (d) from CV slag.

Si and S reduced after leaching. It can suggest that the dissolved Si coated the particles and prevented the further dissolution of Co and Ni after 1hr. This study provides additional evidence of potential application of complexation leaching using organic acids on nickel converter slag; however, selective extraction of target elements should be investigated additionally.

Citric acid and EDTA is an impressive pair for complexation leaching to recover Co and Ni from nickel slag. More research is required to investigate the efficacy of complexation leaching with organic acids, and it is suggested to improve the selectivity toward the target metals by further investigating the complexation leaching. Also, a progression of this work should be to conduct the research on separation and purification. Solvent extraction and precipitation should be especially explored.

CRediT authorship contribution statement

Bona Lim: Software, Investigation, Methodology, Data curation, Writing – original draft. **Richard Diaz Alorro:** Conceptualization, Methodology, Resources, Writing – review & editing, Supervision. **Mark Aylmore:** Formal analysis, Writing – review & editing, Supervision. **David Grimsey:** Resources, Writing – review & editing, Supervision.

Declaration of Competing Interest

The authors declare that they have no known competing financial interests or personal relationships that could have appeared to influence the work reported in this paper.

Data availability

Data will be made available on request.

Acknowledgements

References

Baghalha, M., Papangelakis, V.G., Curlook, W., 2007. Factors affecting the leachability of Ni/Co/Cu slags at high temperature. Hydrometall. 85 (1), 42–52. https://doi.org/10.1016/j.hydromet.2006.07.007.

Bastug, A.S., Gokturk, S., Sismanoglu, T., 2007. 1: 1 Binary complexes of citric acid with some metal ions: Stability and thermodynamic parameters. Rev. Inorg. Chem. 27 (1), 53–65. https://doi.org/10.1515/REVIC.2007.27.1.53.

Coman, V., Robotin, B., Ilea, P., 2013. Nickel recovery/removal from industrial wastes: A review. Resour. Conserv. Recycl. 73, 229–238. https://doi.org/10.1016/j.resconrec.2013.01.019.

Dehaine, Q., Tijsseling, L.T., Glass, H.J., Törmänen, T., Butcher, A.R., 2021. Geometallurgy of cobalt ores: A review. Miner. Eng. 160, 106656.

Goel, S., Pant, K.K., Nigam, K.D.P., 2009. Extraction of nickel from spent catalyst using fresh and recovered EDTA. J. Hazard. Mater. 171 (1–3), 253–261. https://doi.org/10.1016/j.jhazmat.2009.05.131.

Grimsey, E.J., 1992. The Solubility of Cobalt in Fayalite Slags and Factors Affecting Cobalt Recovery. Minerals and Energy Research Institute of Western Australia.

Gunn, G., 2013. Critical Metals Handbook. Wiley.

USGS, 2021. Mineral commodity summaries 2021. U.S, Geological Survey.

Habashi, Fathi., 1993. *A textbook of hydrometallurgy*. Sainte Foy, Quebec: Sainte Foy, Quebec: Métallurgie Extractive Québec.

Huang, F., Liao, Y., Zhou, J., Wang, Y., Li, H., 2015. Selective recovery of valuable metals from nickel converter slag at elevated temperature with sulfuric acid solution. Sep. Purif. Technol. 156, 572–581. https://doi.org/10.1016/j.seppur.2015.10.051.

Ichlas, Z.T., Jones, S.A., Ibana, D.C., Lee, G.-G., Alorro, R.D., 2022. Technospheric mining of scandium from hydrometallurgical tailings of nickel laterite processing: Selection of lixiviant and optimisation of leaching variables. Miner. Eng. 179, 107436 https://doi.org/10.1016/j.mineng.2022.107436.

Johansson, N., Krook, J., Eklund, M., Berglund, B., 2013. An integrated review of concepts and initiatives for mining the technosphere: towards a new taxonomy. J. Clean. Prod. 55, 35–44. https://doi.org/10.1016/j.jclepro.2012.04.007.

Li, Y., Perederiy, I., Papangelakis, V.G., 2008. Cleaning of waste smelter slags and recovery of valuable metals by pressure oxidative leaching. J. Hazard. Mater. 152 (2), 607–615. https://doi.org/10.1016/j.jhazmat.2007.07.052.

Li, Y., Papangelakis, V.G., Perederiy, I., 2009. High pressure oxidative acid leaching of nickel smelter slag: Characterization of feed and residue. Hydrometall. 97 (3), 185–193. https://doi.org/10.1016/j.hydromet.2009.03.007.

Lim, B., Alorro, R.D., 2021. Technospheric Mining of Mine Wastes: A Review of Applications and Challenges. Sustainable Chemistry 2 (4), 686–706. https://doi.org/10.3390/suschem2040038.

Ma, N., Houser, J.B., 2014. Recycling of steelmaking slag fines by weak magnetic separation coupled with selective particle size screening. J. Clean. Prod. 82, 221–231. https://doi.org/10.1016/j.jclepro.2014.06.092.

Markich, Scott J., Brown, Paul L., 1999. Thermochemical data (log K) for environmentally-relevent elements. https://www.osti.gov/etdeweb/servlets/purl/20073871.

Meruane, G., Vargas, T., 2003. Bacterial oxidation of ferrous iron by Acidithiobacillus ferrooxidans in the pH range 2.5–7.0. Hydrometall. 71 (1), 149–158. https://doi.org/10.1016/S0304-386X(03)00151-8.

Nayaka, G.P., Manjanna, J., Pai, K.V., Vadavi, R., Keny, S.J., Tripathi, V.S., 2015. Recovery of valuable metal ions from the spent lithium-ion battery using aqueous mixture of mild organic acids as alternative to mineral acids. Hydrometall. 151, 73–77. https://doi.org/10.1016/j.hydromet.2014.11.006.

Ortego, A., Calvo, G., Valero, A., Iglesias-Émbil, M., Valero, A., Villacampa, M., 2020. Assessment of strategic raw materials in the automobile sector. Resour. Conserv. Recycl. 161, 104968 https://doi.org/10.1016/j.resconrec.2020.104968.

Perederiy, I., Papangelakis, V.G., Buarzaiga, M., Mihaylov, I., 2011. Co-treatment of converter slag and pyrrhotite tailings via high pressure oxidative leaching. J. Hazard. Mater. 194, 399–406. https://doi.org/10.1016/j.jhazmat.2011.08.012.

Prasetyo, A.B., Khaerul, A., Mayangsari, W., Febriana, E., Maksum, A., Andinie, J., Firdiyono, F., Soedarsono, J.W., 2021. Magnesium extraction of ferronickel slag processed by alkali fusion and hydrochloric acid leaching. https://doi.org/10.2298/JMMB200224018P.

Sarker, S.K., Haque, N., Bhuiyan, M., Bruckard, W., Pramanik, B.K., 2022. Recovery of strategically important critical minerals from mine tailings. J. Environ. Chem. Eng. 107622 https://doi.org/10.1016/j.jece.2022.107622.

Shen, Y.F., Xue, W.Y., Li, W., Tang, Y.L., 2008. Selective recovery of nickel and cobalt from cobalt-enriched Ni–Cu matte by two-stage counter-current leaching. Sep. Purif. Technol. 60 (2), 113–119. https://doi.org/10.1016/j.seppur.2007.08.010.

Simandl, G.J., Akam, C., Paradis, S., 2015. Which materials are 'critical' and 'strategic'. Symposium on Strategic and Critical Metals, Victoria, Britihs Columbia.

Smith, R.M., Martell, A.E., 1987. Critical stability constants, enthalpies and entropies for the formation of metal complexes of aminopolycarboxylic acids and carboxylic acids. Sci. Total Environ. 64 (1–2), 125–147. https://doi.org/10.1016/0048-9697(87)90127-6.

Thompson, J.FH., Barnes, S.J., Murray, J., Duke, 1984. The distribution of nickel and iron between olivine and magmatic sulfides in some natural assemblages. Can. Mineral. 22 (1), 55–66.

Wang, Yun, Zhu, Rong, Chen, Qizhou, Wei, Guangsheng, Hu, Shaoyan, Guo, Yaguang., 2018. Recovery of Fe, Ni, Co, and Cu from nickel converter slag through oxidation and reduction. *ISIJ International*: ISIJINT-2018-533. https://doi.org/10.2355/isijinternational.ISIJINT-2018-533.